HHS Public Access

Author manuscript

Int J Cardiol. Author manuscript; available in PMC 2017 March 15.

Published in final edited form as:

Int J Cardiol. 2016 March 15; 207: 326–334. doi:10.1016/j.ijcard.2016.01.016.

Mechanisms Underlying Atrial-Selective Block of Sodium Channels by Wenxin Keli: Experimental and Theoretical Analysis

Dan Hu, MD, PhD[1], **Hector Barajas-Martínez, PhD**[1], **Alexander Burashnikov, PhD**[1], **Brian K. Panama, PhD**[1], **Jonathan M. Cordeiro, PhD**[1], and **Charles Antzelevitch, PhD**[2]

[1]Masonic Medical Research Laboratory, Utica, NY

[2]Lankenau Institute for Medical Research, Wynnewood, PA

Abstract

Introduction—Atrial-selective inhibition of cardiac sodium channel current (I_{Na}) and I_{Na}-dependent parameters has been shown to contribute to the safe and effective management of atrial fibrillation. The present study was designed to examine the basis for the atrial-selective actions of Wenxin Keli.

Methods—Whole cell I_{Na} was recorded at rroom temperature in canine atrial and ventricular myocytes. Trains of 40 pulses were elicited over a range of pulse durations and interpulse intervals to determine tonic and use-dependent block. A Markovian model for I_{Na} that incorporates interaction of Wenxin Keli with different states of the channel was developed to examine the basis for atrial selectivity of the drug.

Results—Our data indicate that Wenxin Keli does not bind significantly to either closed or open states of the sodium channel, but binds very rapidly to the inactivated state of the channel and dissociates rapidly from the closed state. Action potentials recorded from atrial and ventricular preparations in the presence of 5g/L Wenxin Keli were introduced into the computer model in current clamp mode to simulate the effects on maximum upstroke velocity (Vmax). The model predicted much greater inhibition of Vmax in atrial vs. ventricular cells at rapid stimulation rates.

Conclusion—Our findings suggest that atrial selectivity of Wenxin Keli to block I_{Na} is due to more negative steady-state inactivation, less negative resting membrane potential, and shorter diastolic intervals in atrial vs. ventricular cells at rapid activation rates. These actions of Wenxin Keli account for its relatively safe and effective suppression of atrial fibrillation.

Address for correspondence: Charles Antzelevitch, PhD, FHRS, FAHA, FACC, Lankenau Institute for Medical Research, 100 E. Lancaster Ave. Wynnewood, PA 19096, Phone: 484-476-8134, Fax: 484-476-2205, cantzelevitch@gmail.com.

All authors take responsibility for all aspects of the reliability and freedom from bias of the data presented and their discussed interpretation

Author contributions: Charles Antzelevitch and Alexander Burashnikov contributed to the conceptual framework of the study. Brian Panama, Dan Hu, Alexander Burashnikov, Jonathan M. Cordeiro and Hector Barajas-Martínez participated in experimental design, data collection and data analysis. All investigators contributed to drafting and critical revision of the article.

Disclosures: Dr. Antzelevitch received research support from Buchang Pharma, Xi'An, China.

Keywords

Antiarrhythmic drugs; arrhythmias; electrophysiology; pharmacology; atria; ventricles

Introduction

Experimental and clinical studies have demonstrated the value of sodium channel blockers in the management of atrial fibrillation (AF) [1–4]. A major limitation of some sodium channel blockers is their potential proarrhythmic actions in the ventricles. Atrial-selective sodium channel block has recently been advocated as a safe and effective mechanism for termination and suppression of inducibility of AF [1, 5]. The anti-anginal agent, ranolazine, has been shown to be effective in suppressing atrial fibrillation with little effect on peak sodium channel current (I_{Na}) in the ventricle [1]. The atrial-selective effect of ranolazine is largely attributable to differences in the electrophysiological characteristics of sodium channels between atria and ventricle, namely a more negative steady-state inactivation relationship in atria[1].

Wenxin Keli (WK) is a Chinese herb extract that includes 5 main components: the *nardostachys chinensis batal* extract, *codonopsis*, *notoginseng*, *amber*, and *rhizoma polygonati*. Developed in various forms over the past 2000 years, it is used by millions today for the treatment of a variety of cardiac diseases. WK is reported to be of benefit in the treatment of cardiac arrhythmias [5–7], including atrial fibrillation, [8–10] and heart failure [11, 12]. We previously reported that WK exerts atrial-selective inhibition of peak I_{Na} and thus effectively suppresses AF in experimental models of AF [13]. In the present study, we evaluate the nature and kinetics of interaction of WK with the cardiac sodium channel to gain insight into the basis for its atrial selectivity.

Methods

Isolation of adult canine cardiomyocytes

Myocytes were prepared from canine ventricles or atria as previously reported and described in the Online Supplement.

Voltage clamp recordings in cardiomyocytes

Cells were placed in a temperature-controlled chamber (PDMI-2, Harvard Apparatus, Holliston, MA) mounted on the stage of an inverted microscope (Nikon TE300) and recorded using the methods and protocols specified in the Online Supplement.

Cell culture and voltage clamp recordings in HEK293 Cells

HEK 293 cells stably expressing WT-*SCN5A* were transiently transfected with WT-*SCN1B* using Fugene 6. Sodium channel characteristics were studied using whole-cell patch clamp techniques 48 hours after transfection, as described in the Online Supplement [13].

Experimental protocol and theoretical data analysis

Use-dependent inhibition of I_{Na} by WK was measured during trains of 40 pulses to −30 mV following a rest of 15 sec at a holding potential of either −80 mV or −120 mV. To evaluate the effects of rate, the pulse duration was kept constant, and diastolic interval was either 150 ms, 50 ms, or 20 ms. Conversely, the influence of pulse duration was evaluated at constant diastolic interval and pulse durations of 5 ms, 20 ms, or 200 ms. Peak currents in the presence of WK were normalized to I_{Na} measured in the absence of drug. The goal of this experimental protocol was to calculate kinetic binding and unbinding rates of WK with closed, open, and inactivated states of the sodium channel using a guarded-receptor model.[14] Tonic block was determined as the block that develops with the first pulse of a train following a 15 sec rest.

Steady-state inactivation was measured with a standard dual-pulse protocol. Cells were held at −120 mV before evoking a 1-sec conditioning pulse immediately followed by a 20-ms pulse to −30 mV to measure sodium current. Conditioning pulses ranged from −110 to −50 mV and were increased in 10-mV steps. Current was normalized to the peak current recorded after a conditioning step to −120 mV. The normalized current was plotted as a function of conditioning step voltage and fit to a standard Boltzmann function: $1/(1+\exp[(V_h - V)/S_h])$.

The shifts (ΔV_h) of the steady-state inactivation curves by different concentrations (D) of WK were analyzed using Bean's equation[15] to obtain dissociation constants for WK interaction with the inactivated (K_i) and closed (K_c) states of the sodium channel:

$$\Delta V_h = S_h \cdot \ln\left(\frac{1+\frac{D}{K_c}}{1+\frac{D}{K_i}}\right)$$

where S_h is the slope of the steady-state inactivation curve.

Statistical analysis of experimental data

Statistical analysis was performed using a paired Student's *t* test and one-way repeated-measures or multiple comparisons ANOVA followed by Bonferroni's test, as appropriate. All data are expressed as mean ± SD. Statistical significance was assumed at $P<0.05$.

Mathematical modeling

We used a simplified Markovian model for I_{Na} that incorporates the interaction of WK with different states of the channel as previously described.[16] The main theoretical considerations for the development of the model and model equations are shown in the Online Supplement. The number of closed states was reduced to two: the fully closed state and the preopen non-conducting state (see Online Supplement Figure 1). In addition, we assumed that the inactivation process is coupled with activation and requires at least one of four activation gates to open to proceed (Online Supplement Figure 2). The absence of the closed-inactivated state in the Markovian scheme (Online Supplement Figure 1) reflects this fact. In agreement with the experimental data, we shifted the voltage dependence for

intrinsic steady-state inactivation in atrial cells to reproduce the observed approximately 10-mV difference in steady-state inactivation curves between ventricular and atrial cells. Due to the corresponding but smaller (−5 mV) difference in the steady-state activation curves, the inactivation time constant in atrial cells was smaller, in agreement with the experimental data.[17]

Results

Use-dependent effects of WK during trains of pulses

We first examined whether WK interacts strongly with the inactivated state of the sodium channel. Opening of single sodium channels typically occurs in the initial 20 ms of a depolarizing pulse, after which channels enter an inactivated state.[18] If WK has significant interaction with the inactivated state, prolonging the test step during a train of pulses of constant diastolic interval should result in a greater steady-state inhibition of I_{Na}. Figure 1 shows the results of an experiment in which I_{Na} was recorded from atrial and ventricular myocytes using 5 ms and 200 ms pulses to −30 mV separated by 150ms holding at −80 mV. Note that the main effect of WK on peak I_{Na} appears to be tonic block, which was significantly larger in atrial cells than in ventricular cells (Table 1). Similar results were obtained using diastolic intervals of 50 and 20 ms (not shown). The use-dependent effect was much smaller and reached steady-state values after the first pulse. There was no statistically significant difference between the block recorded during the second pulse and the one recorded during the 40^{th} pulse of the train. These results suggest that WK interacts with the inactivated state of the channel and that the rate of binding is very fast. Interestingly, with a holding potential of −120 mV, WK caused relative increases in peak I_{Na} (Supplement Figures 4 and 5).

Next we tested the sensitivity of block to the diastolic interval during a train of pulses of fixed duration. If drug interaction with the closed state is weak, WK will primarily unbind during the “diastolic interval” between test pulses. Abbreviation of the time available for unbinding is expected to result in accumulation of block and greater steady-state inhibition as diastolic interval is reduced. The results of these experiments are presented on Figure 2, which shows a decrease of peak I_{Na} during a train of 200 ms pulses delivered from −80 mV to −30 mV in the presence of 10 g/L WK and normalized to peak I_{Na} recorded during an identical train in the absence of drug (control). We observed very rapid unbinding of WK from the sodium channel at −80 mV, so that the steady-state block was only minimally dependent on the diastolic interval. The unbinding process reached steadystate during the first interpulse interval. As a result, there was no statistically significant difference between the degree of block attained during the second pulse and the one attained during the 40^{th} pulse. Similar results were obtained using other test pulse durations (5 ms and 20 ms, not shown). These results indicate that unbinding of WK from the inactivated sodium channels is very fast.

Finally, we explored the possibility that the tonic block of I_{Na} is due to WK interaction with the closed state of the sodium channel. For this purpose, we employed the same pulse protocols, but using a very negative diastolic (holding) potential of −120 mV. Under these conditions, WK did not produce any noticeable block of I_{Na} (see Supplementary Data)

indicating that WK does not bind to the closed state of the sodium channel and that block is predominantly due to WK interaction with the inactivated state of the channel. If indeed this is the case, WK should shift the steady-state inactivation relationship toward more negative potentials,[15] and this shift should be more pronounced in atrial cells when compared with ventricular cells.

Effect of WK on steady-state inactivation in atrial vs. ventricular cells

These predictions were tested by measuring steady-state availability in control and in the presence of WK (5 g/L and 10 g/L). The results are presented in Figure 3. WK dose-dependently shifted steady-state availability to more negative potentials both in atrial (Figure 3A) and ventricular cells (Figure 3B), with larger effects observed in atrial cells, in agreement with the predictions of the pulse train experiments (Table 1). However, the shift was not as large as expected if WK blocked the pre-open state of the sodium channel, similar to the action of ranolazine[16]. Nevertheless, these shifts were statistically significant and allowed us to calculate dissociation constants of WK with the inactivated and closed states of the sodium channel using Bean's equation.[15] The best fit Bean's function together with the experimental data points (atrial and ventricular data pooled together) are shown in Figure 3C. This analysis yielded the following dissociation constants: K_i = 10.1 g/L and K_c = 1470 g/L. These values support the idea that WK blocks the sodium channel via its interaction with the inactivated state, and at clinically relevant concentrations does not bind to the closed state of the sodium channel.

Effect of WK on steady-state activation in atrial vs. HEK293 cells

In another series of experiments, we examined the effect of WK on steady-state activation of sodium channel current. Application of WK (10 g/L) resulted in no significant shift in the voltage-dependence of channel availability in atrial cells (Control and WK – half activation voltage:: −49.18 ± 1.00 mV vs. −50.68 ± 0.81 mV, n=6, P = 0.27, Figure 4A). Similar results were observed in HEK293 cells stably expressing *SCN5A* (Control, 5 g/L WK and 10 g/L WK- half-activation voltage: −48.00 ± 1.97 mV, −46.67 ± 2.25 mV, and −45.16 ± 2.63 mV, n=4, p=0.27, Figure 4B).

Mathematical model predictions

A mathematical model of WK interaction with the sodium channel was developed based on the assumption that WK interacts predominantly with the inactivated state of the sodium channel, similar to lidocaine, but the kinetic rates are much faster than those of lidocaine, indicating unstable binding. The details of the model are shown in the Online Supplement - Methods. Using this model, we reproduced the experimental voltage clamp protocols using 5, 20, and 200 ms pulses to −30 mV separated by diastolic intervals of 150, 50, and 20 ms at −80 mV. The results of these simulations are shown in Figures 5 and 6, depicting variable pulse durations and variable diastolic intervals, respectively. Results of these simulations were analyzed the same as the experimental data. I_{Na} peaks simulated in the presence of 10 g/L WK were normalized to corresponding peaks of I_{Na} simulated in control conditions. The model predictions shown in Figures 5 and 6 are in good agreement with experimental data shown on Figures 1 and 2, respectively. Numerical comparisons of model predictions and

experimental data are presented in Table 1. The model correctly predicts greater tonic and steady-state block of the atrial sodium channels as compared with the ventricular sodium channels, despite nearly identical rates of WK interaction with a binding site on the alpha subunit. The difference in the amount of block can be explained by the more negative position of steady-state inactivation curve in atrial cells, possibly due to the different ratios of alpha and beta subunits in atrial and ventricular cells.[19] The more negative position of the steady-state inactivation curve in atrial cells results in a larger fraction of inactivated channels that are available for blockade by WK at the normal resting potentials of atrial and ventricular cells.

Next, we simulated the voltage-clamp protocol implemented experimentally to obtain the steady-state inactivation relationship and to study the shift of this curve in the presence of 5 g/L and 10 g/L WK. Figure 7 shows relatively good agreement between the mathematical computer predictions (lines) and experimental data (points), providing support for the hypothesis that the rapid binding and unbinding of WK to/from the inactivated state of the sodium channel with minimal interaction with open and closed states of the channel contributes to the atrial-selective actions.

Computer simulations of the effects of WK

To simulate the effects of WK on the rate of rise of the action potential (AP) upstroke, we utilized AP clamp methods making use of APs recorded experimentally from atrial and ventricular preparations in the presence of 5 g/L WK. The sodium channel model and kinetic rates were adjusted to account for the faster kinetics at 37ºC, i.e. at the temperature used for AP recordings. Figure 8 shows applied AP trains (upper panels) together with simulated upstrokes (middle panels) and the fraction of channels blocked by WK (bottom panels). Shown is the train of APs recorded at a basic cycle length (BCL) of 500 ms at the beginning of the trace followed by acceleration of the pacing protocol to BCL of 300 ms in the middle of the trace, with subsequent return to basic cycle length of 500 ms. The model predicts much greater inhibition of Vmax in atrial vs. ventricular cells at BCL of 300 ms. These computer simulations are consistent with previously published data obtained experimentally using the same protocol (compare with Figure 3 in Burashnikov et al[13]).

Possible contribution of other ions

To assess the possible contribution of ions present in the WK extract, we performed commercial analysis (Avomeen Analytical Services, LLC, Ann Arbor, MI). The concentrations of the following ions were tested: K^+, Ca^{2+}, Na^+, Fe^{2+}, Cd^{2+}, Co^{2+}, Zn^{2+}, F^-, Mn^{2+}, Ba^{2+}, Cs^+, Sr^{2+}. The presence of relatively high concentration of fluoride (6 mg/L) in WK extracts raised concern, especially in light of publications indicating that fluorine (0.1 mg/L to 5 mg/L) can depolarize membrane potential and depresses electrical activity of the guinea pig papillary muscle[20] and cultured cardiomyocytes.[21] Indeed, WK (10 g/L) depolarized the membrane potential by 5–6 mV during AP recordings, which was likely the result of the increased K^+ concentration.

Accordingly, we investigated the possible effects of fluoride (3 mg/L and 20 mg/L) on the AP duration (APD) of coronary-perfused atrial and ventricular preparations and compared

them with those observed in the presence of 5 g/L WK. Figure 9 (right panels) shows that fluoride had no effect on APD or effective refractory period (ERP) in either atrial or ventricular preparations in concentrations as high as 20 mg/L. In contrast, WK produced significant prolongation of atrial ERP while abbreviating atrial and ventricular APD. These results indicate that experimentally observed effects of WK cannot be attributed to the presence of fluoride ions in solutions.

DISCUSSION

The present study delineates the unique characteristics of Wenxin Keli that underlie its actions to suppress AF as demonstrated in experimental models[13] and in the clinic [8–10]. Among the key findings is the demonstration that WK is an inactivated state blocker of the cardiac Na^+ channel. The kinetic rates of WK interaction with atrial and ventricular Na^+ channels are not different, suggesting that atrial and ventricular WK binding sites are similar and do not contribute to the atrial selectivity of WK when evaluated at −120 mV. Surprisingly, at −120 mV WK actually increased the INa. At a holding potential of −80 mV, the reduction in I_{Na} is greater compared to that observed at a holding potential of −120 mV. Intrinsic differences between the APs of atrial and ventricular cells likely play a prominent role. A more negative position of the steady-state inactivation curve in atria,[17, 22, 23] less negative resting membrane potential, and slower phase 3 repolarization giving rise to briefer diastolic intervals in atrial cells than in ventricular cells at fast rates, contribute to the atrial selectivity of many agents displaying atrial-selective inhibition of sodium channel-dependent parameters,[1, 24] and the present study provides support for the hypothesis that this is also the case with respect to WK. These factors, together with rapid dissociation of WK from the sodium channel, are likely responsible for the atrial-selective action of WK to depress I_{Na} and decrease Vmax, as previously reported.[13]

I_{Na} blockers that dissociate rapidly from the sodium channel, including ranolazine, amiodarone and AZD1305, produce atrial-selective depression of sodium channel-dependent parameters and effectively suppress AF in canine coronary-perfused atrial preparations at concentrations that cause little or no effect in the ventricles.[1, 25–28] The atrial selectivity and anti-AF efficacy of these agents has been demonstrated in porcine and canine hearts *in vivo* and *in vitro*.[25–27] Vernakalant also shows atrial-selective I_{Na} block in that it slows conduction velocity in atria, but not in the ventricles, and prolongs atrial ERP largely due to induction of post-repolarization refractoriness (PRR).[29, 30] Dronedarone, a non-iodinated derivative of amiodarone, causes atrial but not ventricular PRR in canine and porcine hearts.[31, 32] The dronedarone-induced PRR is much less pronounced than that of amiodarone. Dronedarone's inhibition of peak I_{Na} is a sensitive function of voltage in guinea pig ventricular myocytes,[32] which may contribute to dronedarone's atrial-selective induction of PRR, owing to the fact that the resting membrane potential (RMP) of atrial cells is less negative than that of ventricular cells.

A number of factors have been shown to underlie the atrial-selective effects of most I_{Na} blockers, including rapid dissociation from the sodium channel, a more negative steady-state inactivation relationship, a more positive RMP, and a more gradual phase 3 of the AP in atrial vs. ventricular cells.[1, 33, 34] The more negative half-inactivation voltage and more

positive RMP importantly reduce the fraction of resting channels in atria vs. ventricles at RMP. Because recovery from sodium channel block generally occurs predominantly during the resting state of the channel, accumulation of sodium channel block is expected to be greater in atria than in the ventricles. The availability of sodium channels may be further reduced by the slight depolarization effected by the elevated levels of K^+ in the WK solution (Figure 8).

Recent studies have shown significant variability in the degree to which sodium channel blockers are atrial-selective.[33–35] Available data suggest that binding affinity of the I_{Na} blocker for a given state of the channel (i.e., open, inactivated, or resting) does not determine the drug's atrial-selectivity.[33] The rate of dissociation of the drug from the sodium channel, however, appears to be a key factor. I_{Na} blockers possessing rapid vs. slow unbinding kinetics tend to be highly atrial-selective (e.g., ranolazine, vernakalant, amiodarone).[16, 17, 24, 33] Agents like flecainide and propafenone, which dissociate relatively slowly from the sodium channel, allow for accumulation of block in both atria and ventricles at rapid rates, leading to absence of atrial-selectivity and in some cases ventricular-predominant effects.[24, 36]

Atrial-selective I_{Na} blockers have been shown to be effective in the clinical management of AF. A number of clinical studies have demonstrated the ability of ranolazine to prevent the induction of AF and to terminate paroxysms of AF using a "pill-in-the-pocket" approach[37, 38]. AZD7009 and AZD1305 have been reported to effectively suppress AF as well.[39, 40] Amiodarone is recognized as the most effective agent for the long-term maintenance of sinus rhythm in patients with AF, although amiodarone has been associated with cardiac as well as non-cardiac toxicity. The combination of ranolazine and dronedarone has been shown to be effective in preventing the induction of AF in experimental models[41] and in significantly reducing the burden of AF in patients with good safety and tolerability. [42]

Atrial-selective I_{Na} blockers generally also inhibit other ion channels (particularly delayed rectifier potassium channel, I_{Kr}). The ability to block I_{Kr} and thus prolong APD has been shown to synergize the effect of these agents to depress I_{Na}.[43] Indeed, any mechanism that causes an increase in atrial APD and slow phase 3 repolarization is expected to synergize the effect of I_{Na} blockers to depress I_{Na} -dependent parameters, thus prolonging ERP and suppressing AF. In the case of WK, the effect of the traditional Chinese medicine (TCM) to prolong the atrial APD in the presence of acetylcholine (ACh), presumably via anticholinergic action, serves this purpose.[13] The prolongation of APD serves to reduce the diastolic interval in atria but not in ventricles at rapid activation rates, thus leading to accumulation of block in atria but not in ventricles.

Study Limitations

The atrial selectivity of Wenxin Keli was determined acutely in "healthy" hearts *ex vivo*. The presence of autonomic influences and other factors present *in vivo* may modulate the effect of Wenxin Keli, resulting in outcomes different from those observed in the present study. [42]

It is important to recognize that cardiac arrhythmias encountered in the clinic are typically associated with electrical and structural abnormalities, which may significantly modulate pharmacological responses, anti-arrhythmic efficacy, and safety. Additional studies are therefore desirable to characterize the effects of Wenxin Keli in pathophysiologic models of AF, particularly in the setting of heart failure. Although it would be of interest to identify and characterize the action of the individual components of Wenxin Keli and their metabolites, the data presented here, in conjunction with previous studies from our group and others, show how this TCM produces atrial-selective sodium channel block resulting in effective suppression of AF. This mechanism is shared by amiodarone, one of the most effective anti-AF agents. However, unlike amiodarone, Wenxin Keli does not appear to have the potential to promote ventricular arrhythmias or to produce significant extra-cardiac toxicity. The unique characteristics of Wenxin Keli identified in the present study should prove helpful in the design of new molecules for safe and effective management of AF.

Supplementary Material

Refer to Web version on PubMed Central for supplementary material.

Acknowledgments

Funding Sources: This study was supported by grants from Buchang Pharma, Xi'An, China; and NIH grant HL-47687 (CA).

We gratefully acknowledge Vladislav V. Nesterenko, Ph.D., for his contribution to computer model development and the expert technical assistance of Judy Hefferon and Robert J. Goodrow Jr.

References

1. Burashnikov A, Di Diego JM, Zygmunt AC, Belardinelli L, Antzelevitch C. Atrium-selective sodium channel block as a strategy for suppression of atrial fibrillation: differences in sodium channel inactivation between atria and ventricles and the role of ranolazine. Circulation. 2007; 116:1449–57. [PubMed: 17785620]
2. Nattel S, Kneller J, Zou R, Leon LJ. Mechanisms of termination of atrial fibrillation by Class I antiarrhythmic drugs: evidence from clinical, experimental, and mathematical modeling studies. J CardiovascElectrophysiol. 2003; 14:S133–S9.
3. Sicouri S, Burashnikov A, Belardinelli L, Antzelevitch C. Synergistic electrophysiologic and antiarrhythmic effects of the combination of ranolazine and chronic amiodarone in canine atria. Circ ArrhythmElectrophysiol. 2010; 3:88–95.
4. Naccarelli GV, Wolbrette DL, Khan M, Bhatta L, Hynes J, Samii S, et al. Old and new antiarrhythmic drugs for converting and maintaining sinus rhythm in atrial fibrillation: comparative efficacy and results of trials. Am J Cardiol. 2003; 91:15D–26D.
5. Minoura Y, Panama BK, Nesterenko VV, Betzenhauser M, Barajas-Martinez H, Hu D, et al. Effect of Wenxin Keli and quinidine to suppress arrhythmogenesis in an experimental model of Brugada syndrome. Heart Rhythm. 2013; 10:1054–62. [PubMed: 23499631]
6. Wang X, Wang X, Gu Y, Wang T, Huang C. Wenxin Keli attenuates ischemia-induced ventricular arrhythmias in rats: Involvement of Ltype calcium and transient outward potassium currents. Mol Med Report. 2013; 7:519–24.
7. Xue X, Guo D, Sun H, Wang D, Li J, Liu T, et al. Wenxin Keli suppresses ventricular triggered arrhythmias via selective inhibition of late sodium current. Pacing Clin Electrophysiol. 2013; 36:732–40. [PubMed: 23438075]

8. Meng Z, Tan J, He Q, Zhu M, Li X, Zhang J, et al. Wenxin Keli versus Sotalol for Paroxysmal Atrial Fibrillation Caused by Hyperthyroidism: A Prospective, Open Label, and Randomized Study. Evid Based Complement Alternat Med. 2015; 2015:101904. [PubMed: 26074982]
9. Kanmanthareddy A, Reddy M, Ponnaganti G, Sanjani HP, Koripalli S, Adabala N, et al. Alternative medicine in atrial fibrillation treatment-Yoga, acupuncture, biofeedback and more. J Thorac Dis. 2015; 7:185–92. [PubMed: 25713735]
10. Chen Y, Nie S, Gao H, Sun T, Liu X, Teng F, et al. The effects of wenxin keli on p-wave dispersion and maintenance of sinus rhythm in patients with paroxysmal atrial fibrillation: a meta-analysis of randomized controlled trials. Evid Based Complement Alternat Med. 2013; 2013:245958. [PubMed: 24368925]
11. Chen Y, Li Y, Guo L, Chen W, Zhao M, Gao Y, et al. Effects of wenxin keli on the action potential and L-type calcium current in rats with transverse aortic constriction-induced heart failure. Evid Based Complement Alternat Med. 2013; 2013:572078. [PubMed: 24319478]
12. Chen Y, Xiong X, Wang C, Wang C, Zhang Y, Zhang X, et al. The effects of wenxin keli on left ventricular ejection fraction and brain natriuretic Peptide in patients with heart failure: a meta-analysis of randomized controlled trials. Evid Based Complement Alternat Med. 2014; 2014:242589. [PubMed: 24868236]
13. Burashnikov A, Petroski A, Hu D, Barajas-Martinez H, Antzelevitch C. Atrial-selective inhibition of sodium channel current by Wenxin Keli is effective in suppressing atrial fibrillation. Heart Rhythm. 2012; 9:125–31. [PubMed: 21884675]
14. Starmer, CF.; Nesterenko, VV.; Undrovinas, AI.; Packer, DL.; Gilliam, FR.; Grant, AO., et al. Characterizing ion channel blockade with the guarded receptor hypothesis. In: Hondeghem, LM., editor. Molecular and cellular mechanisms of antiarrhythmic agents. Mount Kisco, NY: Futura Publishing Co; 1989. p. 179-200.
15. Bean BP, Cohen CJ, Tsien RW. Lidocaine block of cardiac sodium channels. JGenPhysiol. 1983; 81:613–42.
16. Nesterenko VV, Zygmunt AC, Rajamani S, Belardinelli L, Antzelevitch C. Mechanisms of atrial-selective block of Na+ channels by ranolazine: II. Insights from a mathematical model. Am J Physiol Heart Circ Physiol. 2011; 301:H1615–H24. [PubMed: 21821780]
17. Zygmunt AC, Nesterenko VV, Rajamani S, Hu D, Barajas-Martinez H, Belardinelli L, et al. Mechanisms of atrial-selective block of sodium channel by ranolazine I. Experimental analysis of the use-dependent block. Am J Physiol Heart Circ Physiol. 2011; 301:H1606–H14. [PubMed: 21821778]
18. Grant AO, Dietz MA, Gilliam FR III, Starmer CF. Blockade of cardiac sodium channels by lidocaine. Single-channel analysis. CircRes. 1989; 65:1247–62.
19. Gaborit N, Le BS, Szuts V, Varro A, Escande D, Nattel S, et al. Regional and tissue specific transcript signatures of ion channel genes in the non-diseased human heart. J Physiol. 2007; 582:675–93. [PubMed: 17478540]
20. Xiaoxia Y, Jifeng F, Shuliang S. Effects of fluorine and selenium perfusion on the action potential of ventricular cells of guinea pig myocardium [in Chinese]. Chinese JEndemiology. 1995:2–15.
21. Xiaoguang QCL. Effect of fluoride on the spontaneous electrical activities of cultured myocardial cells [in Chinese]. Chinese JEndemiology. 1988:1–10.
22. Li GR, Lau CP, Shrier A. Heterogeneity of sodium current in atrial vs epicardial ventricular myocytes of adult guinea pig hearts. JMolCell Cardiol. 2002; 34:1185–94.
23. Burashnikov A, Di Diego JM, Zygmunt AC, Belardinelli L, Antzelevitch C. Atrial-selective sodium channel block as a strategy for suppression of atrial fibrillation. Ann NYAcadSci. 2008; 1123:105–12.
24. Burashnikov A, Belardinelli L, Antzelevitch C. Atrial-selective sodium channel block strategy to suppress atrial fibrillation: ranolazine versus propafenone. J PharmacolExpTher. 2012; 340:161–8.
25. Burashnikov A, Zygmunt AC, Di Diego JM, Linhardt G, Carlsson L, Antzelevitch C. AZD1305 exerts atrial-predominant electrophysiological actions and is effective in suppressing atrial fibrillation and preventing its re-induction in the dog. J Cardiovasc Pharmacol. 2010; 56:80–90. [PubMed: 20386458]

26. Kumar K, Nearing BD, Carvas M, Nascimento BC, Acar M, Belardinelli L, et al. Ranolazine exerts potent effects on atrial electrical properties and abbreviates atrial fibrillation duration in the intact porcine heart. J CardiovascElectrophysiol. 2009; 20:796–802.
27. Goldstein RN, Khrestian C, Carlsson L, Waldo AL. Azd7009: a new antiarrhythmic drug with predominant effects on the atria effectively terminates and prevents reinduction of atrial fibrillation and flutter in the sterile pericarditis model. JCardiovascElectrophysiol. 2004; 15:1444–50.
28. Szel T, Koncz I, Jost N, Baczko I, Husti Z, Virag L, et al. Class I/B antiarrhythmic property of ranolazine, a novel antianginal agent, in dog and human cardiac preparations. EurJ Pharmacol. 2011; 662:31–9. [PubMed: 21550338]
29. Bechard J, Pourrier M. Atrial selective effects of intravenously administrated vernakalant in conscious beagle dog. J Cardiovasc Pharmacol. 2011; 58:49–55. [PubMed: 21753258]
30. Burashnikov A, Pourrier M, Gibson JK, Lynch JJ, Antzelevitch C. Rate-dependent effects of vernakalant in the isolated non-remodeled canine left atria are primarily due to block of the sodium channel. Comparison with ranolazine and dl-sotaol. Circ Arrhythm Electrophysiol. 2012; 5:400–8. [PubMed: 22322366]
31. Burashnikov A, Sicouri S, Di Diego JM, Belardinelli L, Antzelevitch C. Synergistic effect of the combination of dronedarone and ranolazine to suppress atrial fibrillation. J AmCollCardiol. 2010; 56:1216–24.
32. Bogdan R, Goegelein H, Ruetten H. Effect of dronedarone on Na(+), Ca (2+) and HCN channels. Naunyn Schmiedebergs ArchPharmacol. 2011; 383:347–56.
33. Burashnikov A, Antzelevitch C. Atrial-selective sodium channel block for the treatment of atrial fibrillation. ExpertOpinEmergDrugs. 2009; 14:233–49.
34. Burashnikov A, Antzelevitch C. Atrial-selective sodium channel blockers: do they exist? JCardiovasc Pharmacol. 2008; 52:121–8. [PubMed: 18670368]
35. Burashnikov A, Antzelevitch C. How do atrial-selective drugs differ from antiarrhythmic drugs currently used in the treatment of atrial fibrillation? J Atrial Fibrillation. 2008; 1:98–107.
36. Aliot E, Capucci A, Crijns HJ, Goette A, Tamargo J. Twenty-five years in the making: flecainide is safe and effective for the management of atrial fibrillation. Europace. 2011; 13:161–73. [PubMed: 21138930]
37. Scirica BM, Morrow DA, Hod H, Murphy SA, Belardinelli L, Hedgepeth CM, et al. Effect of ranolazine, an antianginal agent with novel electrophysiological properties, on the incidence of arrhythmias in patients with non ST-segment elevation acute coronary syndrome: results from the Metabolic Efficiency With Ranolazine for Less Ischemia in Non ST-Elevation Acute Coronary Syndrome Thrombolysis in Myocardial Infarction 36 (MERLIN-TIMI 36) randomized controlled trial. Circulation. 2007; 116:1647–52. [PubMed: 17804441]
38. Murdock DK, Reiffel JA, Kaliebe JW, Larrian G. The conversion of paroxysmal of initial onset of atrial fibrillation with oral ranolazine: implications for “pill in the pocket” approach in structural heart disease. J Am CollCardiol. 2010; 55:A6, E58.
39. Geller JC, Egstrup K, Kulakowski P, Rosenqvist M, Jansson MA, Berggren A, et al. Rapid conversion of persistent atrial fibrillation to sinus rhythm by intravenous AZD7009. J ClinPharmacol. 2009; 49:312–22.
40. Ronaszeki A, Alings M, Egstrup K, Gaciong Z, Hranai M, Kiraly C, et al. Pharmacological cardioversion of atrial fibrillation--a double-blind, randomized, placebo-controlled, multicentre, dose-escalation study of AZD1305 given intravenously. Europace. 2011; 13:1148–56. [PubMed: 21561900]
41. Burashnikov A, Sicouri S, Di Diego JM, Belardinelli L, Antzelevitch C. Synergistic effect of the combination of dronedarone and ranolazine to suppress atrial fibrillation. Heart Rhythm. 2010; 1710:1216.
42. Reiffel JA, Camm AJ, Belardinelli L, Zeng D, Karwatowska-Prokopczuk E, Olmsted A, et al. The HARMONY Trial: Combined Ranolazine and Dronedarone in the Management of Paroxysmal Atrial Fibrillation: Mechanistic and Therapeutic Synergism. Circ Arrhythm Electrophysiol. 2015
43. Antzelevitch C, Burashnikov A, Sicouri S, Belardinelli L. Electrophysiological basis for the antiarrhythmic actions of ranolazine. Heart Rhythm. 2011; 8:1281–90. [PubMed: 21421082]

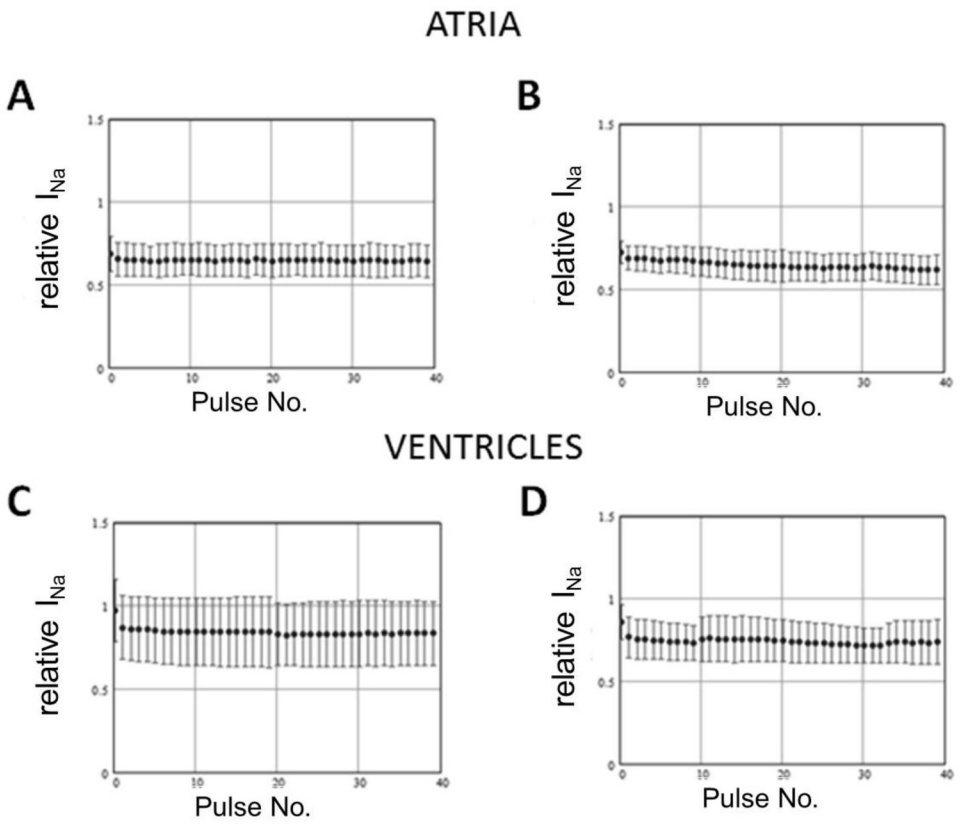

Figure 1.

Rate-dependent inhibition of peak sodium channel current (I_{Na}) in atrial (**A** and **B**, n=4) and ventricular (**C** and **D**; n=5) cells in response to trains of pulses, −80 mV to −30 mV, 5 (**A** and **C**) or 200 ms (**B** and **D**) duration delivered with a diastolic interval of 150 ms, in the presence of 10 g/L Wenxin Keli. Peak I_{Na} recorded in the presence of Wenxin Keli was normalized to peak I_{Na} recorded during the same trains under control conditions.

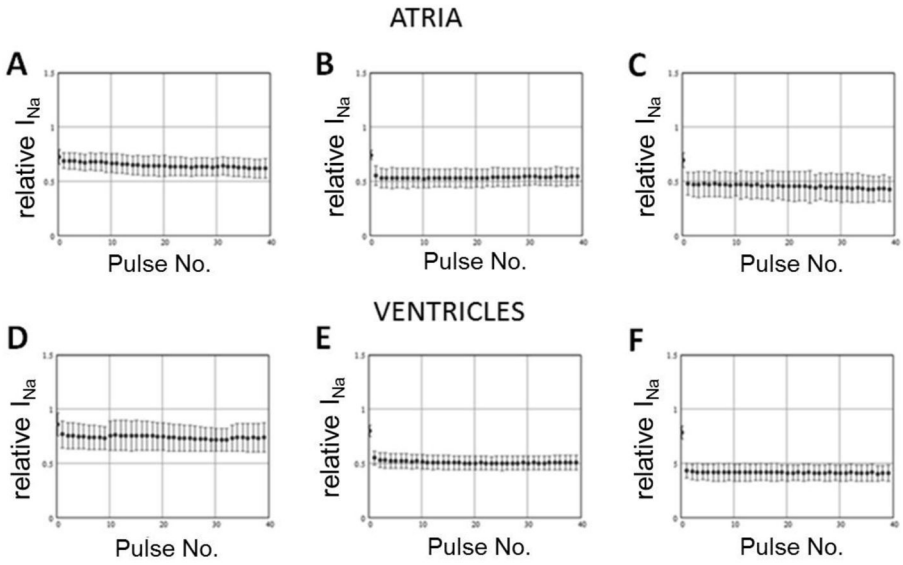

Figure 2.

Decrease of the peak sodium channel current (I_{Na}) during the train of 200 ms pulses delivered from −80 mV to −30 mV in the presence of 10 g/L Wenxin Keli and normalized to peak I_{Na} recorded during the same train in control conditions. Data obtained in atrial cells (top panels; n=4) and in ventricular cells (bottom panels; n=5) using interpulse intervals of 150 ms (**A** and **D**), 50 ms (**B** and **E**), and 20 ms (**C** and **F**).

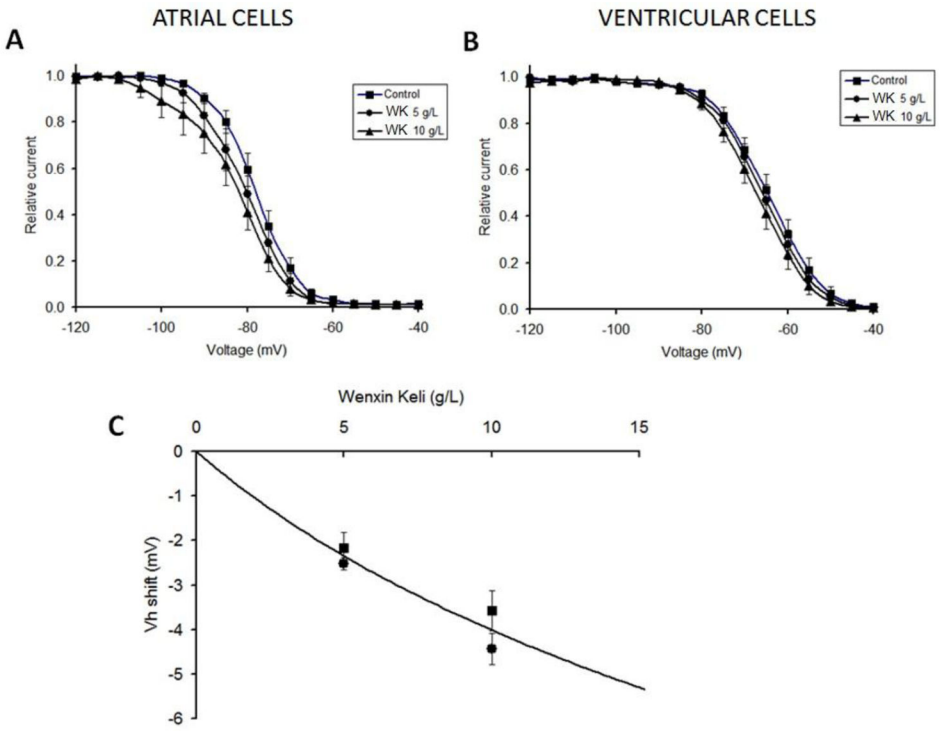

Figure 3.

Effect of Wenxin Keli (WX) on sodium channel availability. Shift of $h_{\infty}(V)$ in the presence of 5 g/L (circles) and 10 g/L WK (triangles) recorded in atrial cells (**Panel A**) and in ventricular cells (**Panel B**). **Panel C** shows the experimentally recorded values of the shift of $h_{\infty}(V)$ in atrial cells (circles) and ventricular cells (squares) together with the best fitted "Bean's" function[15] (solid line), yielding dissociation constants for WK interaction with the closed state of the channel (~1500 g/L) and with the inactivated state of the channel (~10 g/L).

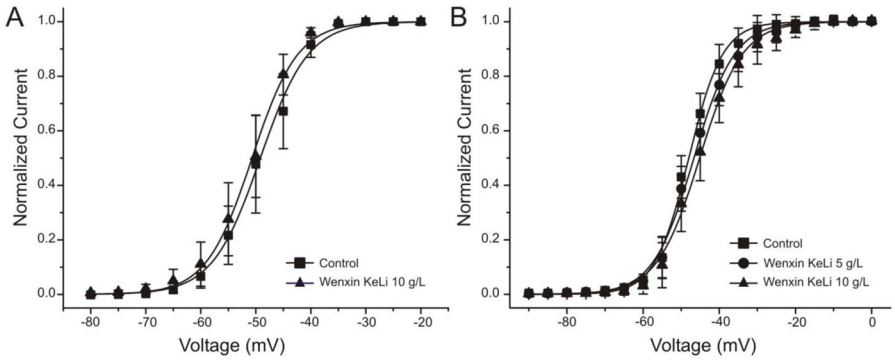

Figure 4.

Effect of Wenxin Keli (WX) on sodium channel activation. There is no change of $V_{1/2}$ in the presence of 5 g/L (circles) and 10 g/L WK (triangles) recorded in canine atrial cells (**Panel A**) and in HEK293 cells expressed with sodium current (**Panel B**).

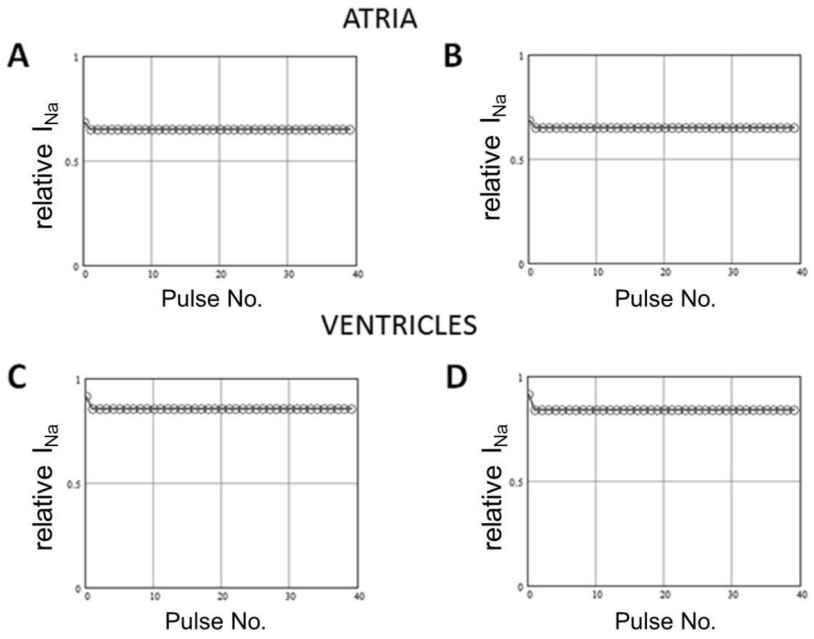

Figure 5.

Computer simulated decrease of the peak sodium channel current (I_{Na}) during the train of pulses (5 and 200 ms duration) delivered from −80 mV to −30 mV in the presence of 10 g/L Wenxin Keli using diastolic interval of 150 ms. Peaks of I_{Na} simulated in the presence of Wenxin Keli were normalized to peaks of I_{Na} simulated during the same trains in control conditions. Data were simulated using an atrial sodium channel model (top panels; n=4) and using a ventricular sodium channel model (bottom panels; n=5) using pulse durations of 5 ms (**A** and **C**) and 200 ms (**B** and **D**). Compare with Figure 1.

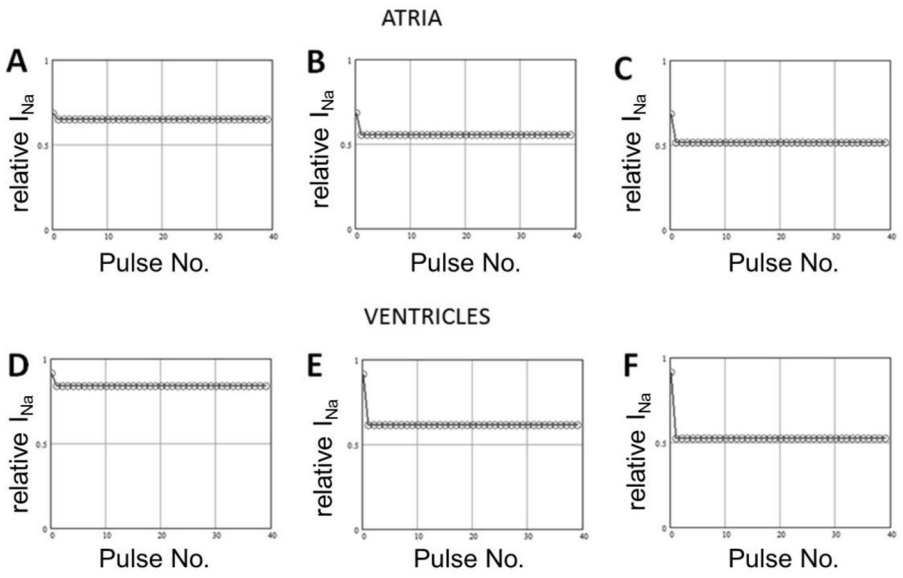

Figure 6.

Computer simulation of decrease in peak sodium channel current (I_{Na}) during trains of 200 ms pulses delivered from 80 mV to 30 mV in the presence of 10 g/L Wenxin Keli and normalized to peak I_{Na} simulated during the same train in control conditions. Data were simulated using an atrial sodium channel model (top panels; n=4) and a ventricular sodium channel model (bottom panels; n=5) using interpulse intervals of 150 ms (**A** and **D**), 50 ms (**B** and **E**), and 20 ms (**C** and **F**). Compare with Figure 2.

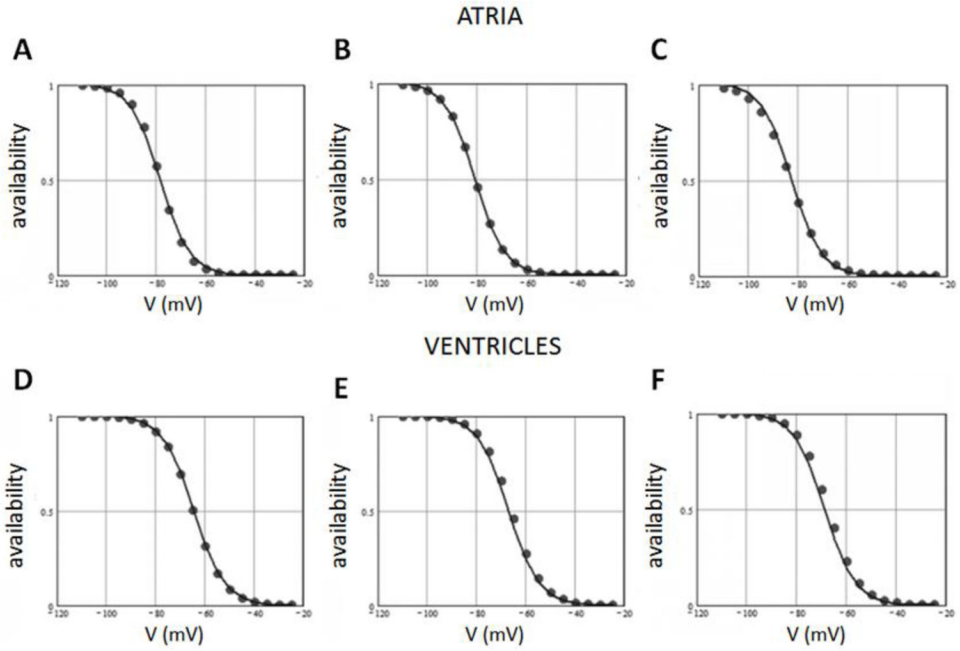

Figure 7.

Comparison of experimentally recorded (data points) and model-generated (lines) steady-state inactivation in atrial (top panels) and ventricular cells (bottom panels) in control (**A** and **D**) and in the presence of 5 g/L (**B** and **E**) and 10 g/L (**C** and **F**) Wenxin Keli.

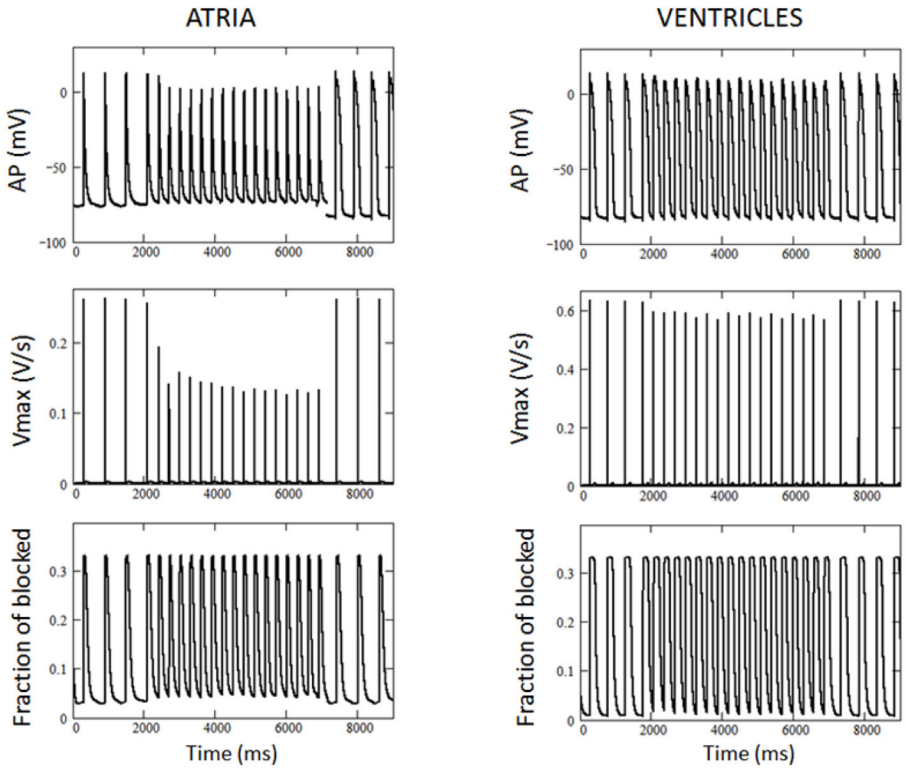

Figure 8.

Simulation of I_{Na} block by Wenxin Keli using action potential (AP) clamp at 37°C. Trains of APs experimentally recorded from ventricular (right) and atrial (left) cells were applied as a command potential to simulate additional block of I_{Na} by 5 g/L Wenxin Keli after basic cycle length was changed from 500 to 300 ms in ventricular and atrial cells. From top to bottom: Atrial or ventricular APs, simulated open state probability (~V_{max}) and fraction of blocked channels.

A

Analyte	Concentration (μg/L)	Concentration (mmol/L)
Barium	<100	<0.0007
Cadmium	<0.2	<2 x 10^{06}
Calcium	1900	0.047
Cesium	<2	<2 x 10^{05}
Cobalt	<10	<0.0002
Fluoride	6000	0.3
Iron	90	0.002
Manganese	30	0.0006
Potassium	23000	0.59
Sodium	16000	0.70
Strontium	<50	<0.0006
Zinc	40	0.0006

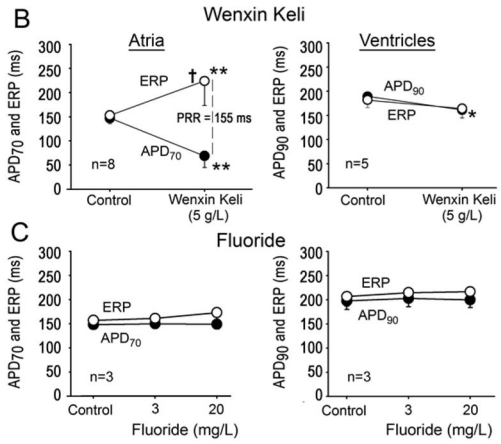

Figure 9.

Panel A shows the partial ionic composition of Wenxin Keli solution (10 g/L) indicating the presence of relatively high concentration of fluorine ions. **Panels B** and **C** compare the effects of Wenxin Keli (5 g/L) and fluorine (3 and 20 mg/L) on atrial and ventricular action potential duration (APD) and on effective refractory period (ERP), and post-repolarization refractoriness (PRR) at a cycle length of 500 ms. Dashed lines depict the duration of PRR. PRR was approximated by the difference between ERP and APD measured at 70% (APD_{70}) in atria, and between ERP and APD measured at 90% repolarization (ADP_{90}) in ventricles. Note that ERP corresponds to APD measured at 70–75% repolarization ($ADP_{70–75}$) in atria and to APD_{90} in ventricles. * - $p<0.05$ vs. control. ** - <0.001 vs. control. † - $p<0.001$ vs. APD_{70}. **Panel B** is modified, with permission, from Burashnikov et al.[4]

Table 1

Effects of Wenxin Keli on the sodium channel. Experimentally-derived parameters vs. mathematical model predictions.

	Experimental data		Model predictions	
	Atrial	**Ventricular**	**Atrial**	**Ventricular**
Tonic block (5 g/L, −80mV)	0.88 ± 0.06	1.01 ± 0.02	0.81	0.95
Tonic block (10g/L, −80mV)	0.74 ± 0.03	0.93 ± 0.04	0.68	0.91
Use-dependent block (150 ms)	0.62 ± 0.08	0.74 ± 0.13	0.64	0.84
Use-dependent block (20 ms)	0.42 ± 0.08	0.48 ± 0.15	0.45	0.52
V_h shift (mV), 5 g/L	−2.52 ± 0.14	−2.16 ± 0.34	−2.45	−2.36
V_h shift (mV), 10 g/L	−4.43 ± 0.35	−3.58 ± 0.45	−4.18	−3.98

Tonic = remaining current relative to control due to tonic block (1^{st} pulse in train)

Use-dependent = remaining current relative to control due to use-dependent block (40^{th} pulse in train)